

# Determination of Parameters of Porous Structure Affecting the Release Mechanisms of Long-Lived Radionuclides from Irradiated Graphite in Contact with Liquid Media

A. O. Pavlyuk<sup>a</sup>, S. G. Kotlyarevskii<sup>a</sup>, R. I. Kan<sup>a</sup>, A. G. Volkova<sup>b</sup>, D. A. Zolotov<sup>c</sup>,  
A. V. Pakhnevich<sup>d,e</sup>, E. V. Zakharova<sup>b</sup>, and A. A. Shiryaev<sup>b,\*</sup>

<sup>a</sup> Pilot and Demonstration Center for Decommissioning of Uranium-Graphite Nuclear Reactors,  
Seversk, Tomsk oblast, 636000 Russia

<sup>b</sup> Frumkin Institute of Physical Chemistry and Electrochemistry, Russian Academy of Sciences, Moscow, 119071 Russia

<sup>c</sup> Shubnikov Institute of Crystallography, Federal Scientific Research Center “Crystallography and Photonics,”  
Russian Academy of Sciences, Moscow, 119333 Russia

<sup>d</sup> Borisyak Paleontological Institute, Russian Academy of Sciences, Moscow, 117997 Russia

<sup>e</sup> Frank Laboratory of Neutron Physics, Joint Institute of Nuclear Research, Dubna, Moscow oblast, 141980 Russia

\*e-mail: a\_shiryaev@mail.ru

Received November 5, 2019; revised December 21, 2019; accepted December 28, 2019

**Abstract**—Specific features of the porous structure of irradiated and virgin reactor graphite of Russian brands have been analyzed. The porosity parameters affecting the leaching of radionuclides from graphite radioactive waste (RAW) were determined: fraction of open porosity, distribution of pore throat cross-sections, surface of open pores. The volume of open pores accessible for leaching aqueous media in the irradiated graphite was estimated. A model describing the leaching of radionuclides from irradiated graphite accounting for the porosity contribution is proposed. The parameters that numerically characterize the resistance of graphite RAW against leaching and are independent of the geometric shapes of separate fragments (samples) were determined.

**Keywords:** irradiated graphite, porous structure, pore distribution, open porosity, leaching of radionuclides

**DOI:** 10.1134/S1066362220060089

## INTRODUCTION

At present more than 100 energy-producing and industrial uranium-graphite reactors (UGRs) exist; mostly they are situated on the territory of the Russian Federation, France, Great Britain, United States. Most of reactors of this type are shut down. In the nearest 20 years it is planned to shut down the power units with UGRs remaining in service. The total mass of irradiated graphite (blocks, bushings, debris, etc.) accumulated in the Russian Federation as a result of operation of industrial (IUGRs) and energy-producing UGRs is about 60 thousand tons. At present, the problem of their disposal is actively discussed [1]. The problem of handling the irradiated graphite remains topical not only in Russia, since commonly accepted regulations do not allow dispatching graphite into the existing disposal sites of the radio-

active waste (RAW) without preliminary deactivation to diminish the content of long-lived radionuclides (the acceptance criteria are not implemented in all countries) [2]. In the international project GRAPA, organized by IAEA in cooperation with specialists from the RF, the analysis of the properties of graphite and technologies of handling this material continues in order to develop practical recommendation to solve the problem [3]. A considerable number of studies aimed to investigate properties of the graphite, especially the analysis of the leaching from Western graphite brands, have been carried out under the European project CAST, the main results of which have been published in a special issue of Radiocarbon journal [4].

The potential hazard of the main mass of graphite RAW (~95%) is determined by the presence of predominantly long-lived radionuclides <sup>14</sup>C and <sup>36</sup>Cl.

A fraction of the graphite contains a significant amount of isotopes from fuel (actinides and fission products), which determine the potential hazard of this type of the graphite RAW. The  $^{14}\text{C}$  isotope (half-life  $5.37 \times 10^3$  yr) is a radionuclide dominant in specific activity. Its specific activity in the graphite from Russian UGRs is  $10^4$ – $2.5 \times 10^6$  Bq/g. For  $^{36}\text{Cl}$  (half-life  $3.1 \times 10^5$  yr), the specific activity varies within the range  $10^1$ – $2 \times 10^3$  Bq/g.

One of distinctive features of irradiated graphite as a type of RAW is its developed porous structure, absent in other kinds of RAW (vitrified, ceramic, etc.). The porosity of graphite strongly affects both the spatial distribution of radionuclides during operation of a reactor and the release of radionuclides from graphite in contact with external media at various handling stages. Results of investigation of the accumulation and distribution of radionuclides in irradiated graphite show that a complex pattern of contamination with radionuclides is formed in graphite during the reactor operation. Its formation is affected both by the operation routines and by structural features of the graphite and, in particular, by properties of the porous structure (volume of open porosity, set of communicating pore channels, distribution of pore throat cross-section, etc.). It should be noted that the developed porous structure of graphite RAW can strongly affect the release pattern of radionuclides from the irradiated graphite at various stages of its handling, including storage [6], disposal, and liquid and/or thermal deactivation [7–9].

## RESULTS

**Peculiarities of formation of the bulk content of the principal long-lived radionuclides under operation conditions in UGRs.** The graphite stacks of domestic UGRs operate(d) either in the atmosphere of nitrogen gas (IUGR, AMB, AM) or in the nitrogen-helium atmosphere (RBMK). The gas fills all the hollows in the graphite stack, including gaps between graphite pieces, and also the whole volume of the open porosity. The specific features of  $^{14}\text{C}$  accumulation in graphite were considered in [7, 10]. It was noted that a considerable amount of  $^{14}\text{C}$  (50–80%) is formed according to reaction  $^{14}\text{N}(n,p)^{14}\text{C}$  from nitrogen gas and is fixed in the near-surface layer of graphite parts, walls of open pores, and surface of graphite crystallites accessible to gaseous nitrogen.

According to calculations, the depth to which  $^{14}\text{C}$  recoil nuclei are implanted may be as large as 150–

200 nm with an average value of 90–130 nm [1]. It is noteworthy, however, that the displacement energy of a carbon atom in graphite decreases from 24 to 5 eV as the amount of radiation defects grows [12] and the irradiation temperature is raised [13]. Thus, the depth of  $^{14}\text{C}$  implantation into graphite grains will depend both on the total irradiation time of the material and on the operational temperature. In any case, the penetration depth of implanted nuclei markedly exceeds characteristic dimensions of graphite crystallites. Note that the values obtained refer to the implantation of recoil nuclei from any surface (outer surface of an irradiated detail, pore wall surface, etc.).

This effect has been experimentally confirmed by investigation of change in the  $^{14}\text{C}$  content of in the surface layer of a graphite block from RBMK of power unit no. 2 of Leningrad nuclear power plant. The  $^{14}\text{C}$  content was determined in layers mechanically removed from the block surface (Fig. 1). For a thin surface layer (with thickness  $<0.05$  mm) the surface area of the graphite block itself dominates over the surface of open pores in this thin layer, and the effect of an increased specific (per unit mass) content of the isotope on the surface of an irradiated block is noticeable. As the thickness of the removed layer increases, its specific content of  $^{14}\text{C}$  will be largely determined by the activity of the isotope localized at the pore walls, and the effect of an increased activity on the surface of the graphite block will be less noticeable.

There are two main sources of chlorine in virgin graphite. First, chlorine is present in the starting components used to produce graphite - petroleum coke and cake binder, and partly remains in the final product after the annealing at 1000–1300 °C. In addition, chlorine-containing reagents are used in gas purification of graphite at the final stage of the production cycle. Neutron activation, mostly by the reaction  $^{35}\text{Cl}(n,\gamma)^{36}\text{Cl}$ , is the second important source. The residual content of chlorine is due to its localization in structural features in graphite (closed pores, crystallite boundaries) poorly accessible for the environment, including the contact fluid in leaching tests. The experimental and theoretical studies of the distribution and content of  $^{36}\text{Cl}$  in graphite [14] revealed a significant scatter of the  $^{36}\text{Cl}$  specific activity over the volume of the graphite stack (nugget effect). It can be assumed that the heterogeneity of the chlorine spatial distribution is largely due to the inhomogeneity of the microstructure of the starting

reactor graphite resulting from its high porosity. The porosity strongly affects the volume diffusion of  $^{36}\text{Cl}$  (or  $^{35}\text{Cl}$  parent atoms) in graphite and their retention in structural features of the material in fabrication and/or in its operation in UGRs.

Thus, it can be stated that the porous structure of graphite largely determines the specific features of the spatial distribution, mechanisms (strength) of retention of the most long-lived radionuclides (and/or of their physicochemical forms) in the structure of graphite articles in the stacks of UGRs.

**Features of the porous structure of irradiated graphite and its effect on the leaching of the main long-lived radionuclides.** An important peculiarity of the irradiated reactor graphite, which distinguishes it from many kinds of solid RAW, is its comparatively high porosity. Properties of the porous structure of irradiated graphite depend on its brand and history of irradiation of particular graphite parts in UGR stacks. The graphite brands differ in the starting raw material, types and sequence of technological steps during production (with or without impregnation with petroleum pitch), parameters of individual technological procedures, etc. [15]. The data of small-angle X-ray scattering (SAS), diffraction, and permeability measurements were used to demonstrate that the general tendency of changes in the porous structure of graphite under irradiation is that the fraction of the open-pore volume decreases due to the partial closure of pores and, accordingly, the share of the closed porosity increases [5, 15, 16]. It is noteworthy, however, that the interpretation of SAS data in the above-mentioned studies is not unambiguous. Studies of the porous structure of reactor graphite by X-ray tomography demonstrate that open pores form a developed 3D network connected by channels with irregular cross-section [17, 18]. These conclusions suggest that a through impregnation (filling of the open-pore volume) of bulk graphite fragments with leaching liquid is, in principle, possible.

The following factors related to the developed porous structure can affect the process of  $^{14}\text{C}$  and  $^{36}\text{Cl}$  leaching from graphite RAW:

- it is necessary to take into account the peculiarities of the spatial distribution and retention mechanisms of  $^{14}\text{C}$  and  $^{36}\text{Cl}$  and, accordingly, the presence of various species in irradiated graphite;

- the process of  $^{14}\text{C}$  and  $^{36}\text{Cl}$  leaching may proceed largely by volume mechanism, rather than by the

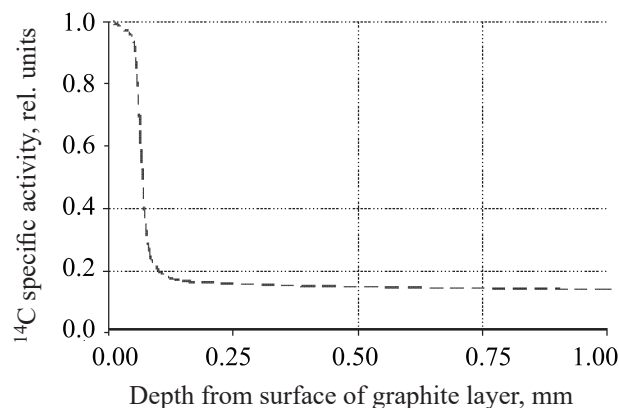


**Fig. 1.** Typical distribution of the  $^{14}\text{C}$  activity in the surface layer of a graphite block from RBMK-1000 reactor at Leningrad nuclear power plant.

surface one (as in the case of a monolithic material), since the pore area accessible to the leaching agents may substantially exceed the geometric surface area of fragments of real graphite RAW;

- analysis of the leaching process requires consideration not only of the external surface area of graphite samples (parts and fragments), but also of the surface of pore channels. Thus, the area of contact with the leaching solution depends on the volume fraction of the open porosity of graphite and the pore throat cross-section distribution (effective radius).

Stabilisation of the leaching of radionuclides from graphite samples may occur much later than in case of RAW samples with monolithic structure due to slower penetration and propagation of the solution through the porous structure of graphite and the limited rate of mass exchange with the solution. Sorption/desorption of radionuclides from solution in the course of motion *via* the pores to the sample surface are also possible.

In accordance with the standards commonly used in the RF to determine the leaching rate [19, 20], the main parameter that characterizes the stability of a material against leaching and is independent of the geometric shape of a sample (fragment) is the leaching rate related to the geometric area of a sample or fragment [Eq. (1)]:

$$R_n^i = \frac{a_n^i}{A^i F_0 t_n}, \quad (1)$$

where  $R_n^i$  is the rate of leaching of  $i$ th radionuclide during  $n$ th leaching period, related to the geometric surface area

of a sample or fragment,  $g/(cm^2 \cdot day)$ ;  $a_n^i$  is the activity of  $i$ th radionuclide that passed into solution during the  $n$ th period of leaching, Bq;  $A^i$  is the specific activity of  $i$ th radionuclide in graphite, Bq/g;  $F_0$  is the geometric surface area of a sample or fragment,  $cm^2$ ; and  $t_n$  is the duration of  $n$ th period of leaching, days.

When analyzing expression (1), we note that, although the parameter  $R_n^i$  characterizes the stability of irradiated graphite against leaching of radionuclides, it depends on the geometric shape of a sample because this expression disregards the porosity. However, this GOST (State Standard) has been developed for solid RAWs (in fact, monolithic samples), and only the external surface area is taken into account when calculating the leaching rate. In the case of a porous material, to which category belongs irradiated graphite, it is also necessary to take into account the area of internal surfaces accessible for the leaching medium.

Presumably, as the solution fills all the accessible hollows in graphite (pores, intercrystallite spaces, etc.), the effective leaching surface area and the rate of the mass exchange with the leaching solution are stabilized. Also, the rates of sorption/desorption of radionuclides in the course of pore-mediated flow to the sample surface attain equilibrium. Further, the leaching dynamics becomes monotonic and gradually decreases.

After the stable leaching mode is attained, the effective leaching surface area is given by the expression

$$F_{\text{eff}} = F_0 + F_S, \quad (2)$$

where  $F_{\text{eff}}$  is the effective leaching surface area of a sample,  $cm^2$ ;  $F_0$  is the geometric surface area of the sample,  $cm^2$ ; and  $F_S$  is the surface area accessible to the solution (open pores, intercrystallite spaces, etc.),  $cm^2$ .

In this case, the parameter characterizing the stability of graphite RAW will be the leaching rate of a radionuclide, related to the effective leaching surface area (effective leaching rate  $R_{\text{eff}}$ ). The value of  $R_{\text{eff}}$  is given by

$$R_{\text{eff}}^i = \frac{a_n^i}{A^i (F_0 + F_S) t_n}, \quad (3)$$

where  $R_{\text{eff}}^i$  is the leaching rate of  $i$ th radionuclide during  $n$ th period of leaching, related to the effective leaching surface area,  $g/(cm^2 \text{ day})$ .

If the total volume of open pores is accessible for filling by the contact solution,  $F_S$  is taken to be equal

to the total geometric surface of open pores in a sample. The parameter  $R_{\text{eff}}$  will be independent of the geometric characteristics of the sample, and determines the stability of a material being tested against leaching of radionuclides in relation to specific features of their spatial distribution in the structure of graphite, strength of retention of radionuclides (and related compounds) in graphite, and their ability to form water-soluble forms.

Thus, it follows from Eqs. (2) and (3) that an analysis of the structural features of the porous structure of irradiated and virgin reactor graphite of Russian brands is necessary. This analysis will allow to determine a set of parameters that affect the leaching of radionuclides from graphite RAW: share of the open porosity, pore throat distribution function, surface of open pores, and also to estimate the accessibility of open pores in irradiated graphite to leaching solutions. The present study reports results of investigation of porosity of samples of a real irradiated graphite from UGRs.

**Results of studies of the porous structure of irradiated and virgin reactor graphite of domestic brands and determination of parameters of this structure that affect the leaching of radionuclides from graphite RAWs.** In the present study the porous structure of virgin and irradiated graphite of Russian brands was studied: block graphite of GR-220 brand (used in IUGRs), bushing graphite GR-26 (used in IUGRs), and hard contact ring (KTK) graphite GR-93 (used in RBMKs). The total volume fraction of pores ( $v$ ) was determined from analysis and processing of tomographic images of the samples, obtained with a SkyScan 1172 instrument. To obtain a representative pattern, samples with dimensions of up to  $4 \times 8$  mm were examined with a spatial resolution of  $7.4 \mu\text{m}/\text{pixel}$ . The porosity was evaluated by the general algorithm comprising several main stages: determination of sample boundaries, calculation of the total sample volume from tomographic cross-sections, segmentation of individual pores, and subsequent calculation of the ratio of the obtained volumes for each cross-section. This approach was described in detail in [21]. Representative examples of analysis and processing of the reconstructed tomographic images are shown in Figs. 2 and 3. The results of determination of the volume fraction of pores in the studied samples are combined in Table 1. For several samples the volume of open pores accessible for saturation in aqueous medium. Experiments were performed by impregnation with water following



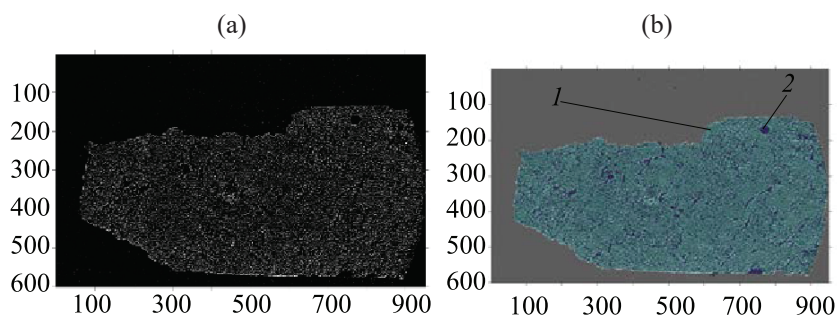


**Fig. 2.** Result of segmentation of a tomographic cross-sectional image of irradiated GR-220 graphite. (a) Example of a restored tomographic slice, (b) result of segmentation: (1) main volume and (2) volume containing pores/inclusions.

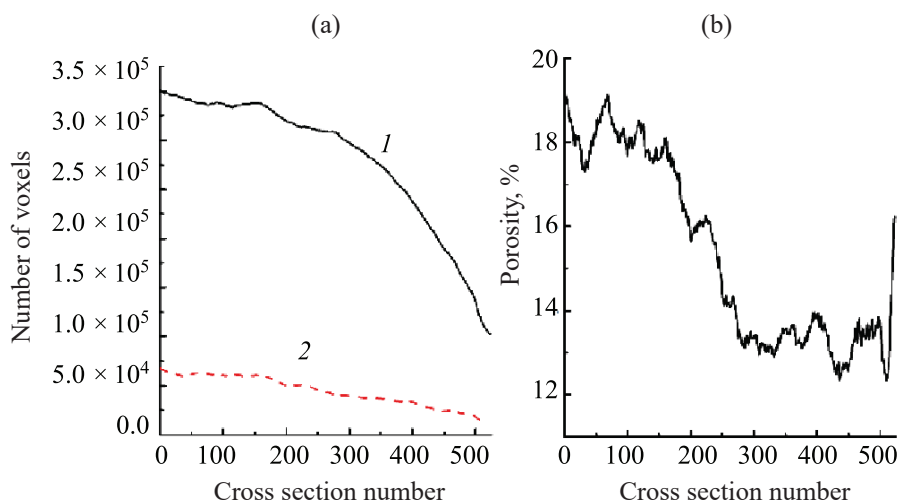


**Fig. 3.** Result of processing of the tomographic slices of a sample of irradiated GR-220 graphite and determination of the open porosity volume. (a) Dependence of the volume of material (1) and pores (2) on the number of a tomographic cross-section and (b) porosity in various tomographic cuts.

procedure described in [22]. The samples were kept in an aqueous medium under normal conditions for 30 days. The results are combined in Table 2.

Figure 4 presents the evolution of the fraction of open porosity under irradiation in bushing graphite GR-76 in IUGR and in experimental graphite produced by the similar technology, but with impregnation with petroleum pitch. The results of experiments and data on the history of irradiation of bushings are used.

Comparison of values of the total and open porosities obtained by two independent methods (X-ray tomography and impregnation with water, Tables 1 and 2) show that for irradiated and virgin GR-220 and GR-76 graphites these characteristics are rather similar, indicating insignificant fraction of closed pores. Certain differences between the values obtained by these analytical methods are probably due both to the scatter of properties of individual samples and to the fact that

information about pores with diameter smaller than 4–5  $\mu\text{m}$  is lost in the current tomographic experiment. Consequently, nearly the total pore volume in the whole volume of graphite samples, including deep regions, is accessible for saturation with aqueous solutions. Thus, the experimental results of the present study confirm the conclusion formulated in [17], according to which

**Table 1.** Volume fraction of pores in graphite of various brands obtained using X-ray tomography

Characteristics of samples (brand irradiation)	Volume fraction of pores $v$ , %
GR-220 (irradiated)	15.338
GR-220 (virgin)	18.367
GR-76 (irradiated)	16.746
GR-93 (virgin)	16.102

**Table 2.** Volume fraction of pores in graphite of various brands obtained by impregnation with water

Characteristics of samples (brand, irradiation, amount)	Fraction of open pores accessible for saturation with water, %
GR-220 (virgin), 10 samples	18–22
GR-220 (irradiated), 1 sample	17.1 <sup>a</sup>
GR-76 (virgin), 25 samples	17–23
GR-76( irradiated), 5 samples	15–20
Experimental bushing graphite impregnated with petroleum pitch (virgin), 25 samples	12–18
Experimental bushing graphite impregnated with petroleum pitch (irradiated), 7 samples	11–14

<sup>a</sup> The volume content of water in a graphite core (diameter ~8 mm, length ~57 mm) measured by keeping in water at room temperature for 1.5 years.

the open pores in the bulk of graphite form a common volume in the form of a developed 3D network of interconnected channels. The impregnation with water of the porous structure of graphite samples is, in fact, the process of air displacement and filling with water of a system of communicating vessels.

The irradiation in a reactor (for the example of samples of block and bushing graphite of GR-220 and GR-76 brands) during the whole operation period leads to an insignificant decrease in the porosity volume (Tables 1 and 2, Fig. 4). With allowance for the initial scatter of the fraction of open porosity between individual samples, it was shown that for GR-220 block graphite the volume of the open porosity decreases by 15–25 rel % during the whole service period of a reactor, and, for GR-76 bushing graphite (irradiation duration ~9 years), the decrease is 5–15 rel %.

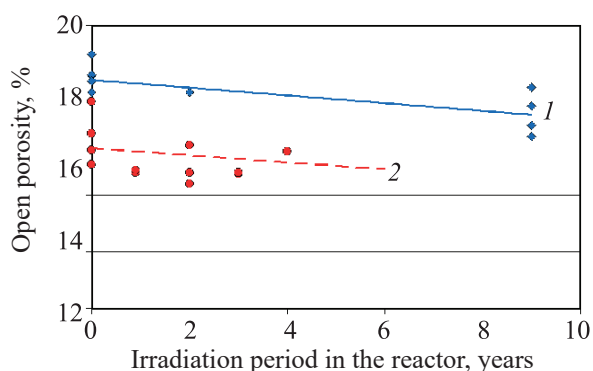


**Fig. 4.** Dynamics of changes of the open porosity fraction for (1) bushing graphite GR-76 and (2) experimental bushing graphite (produced by technology close to that for GR-76 graphite, but with impregnation with petroleum pitch) under irradiation in IUGR.

A calculation of the pore throat radii distribution for open pores from tomographic data is more complicated and can be performed by various methods. In our study the algorithm comprising the following main steps was used: (1) binarization of the volume of pores/inclusions; (2) search for separate pores/inclusions (average number of pores in a single cross-section was  $5 \times 10^3$ ); (3) determination of the coordinate of position for each pore/inclusion and maximum radius of an inscribed circle. Results obtained in a search for pores and determination of their maximum throat radius in a single cross-section of a sample are presented in Fig. 5. The results of a processing of this kind for all the cross-sections were used to plot histograms of maximum radii of pores and to calculate average values for all four samples (Fig. 6).

After the tomographic analysis the samples were studied by the small-angle X-ray scattering (SAXS) using a dedicated diffractometer SAXSess. The measurements were performed in vacuum in a quasi-point configuration with monochromatic  $\text{CuK}_\alpha$  radiation at scattering vectors  $q$  of 0.25 to  $27 \text{ nm}^{-1}$ . Several studies are known in which Russian reactor graphites were examined by the SAXS method [23,24]. In these works the SAXS signal was attributed to the scattering on pores. However, other nanoscale heterogeneities, e.g., dislocation loops and clusters of point defects, may also contribute to the scattering. Figure 7 presents SAXS curves for the samples under study. For the bushing graphite the scattering intensity decays rather uniformly [11]. There is no obvious straight region in Guinier plot ( $\log I - q^2$ ), which is indicative of the polydispersity of scatterers. A calculation of the size distribution of the heterogeneities gives a rather wide range of values:

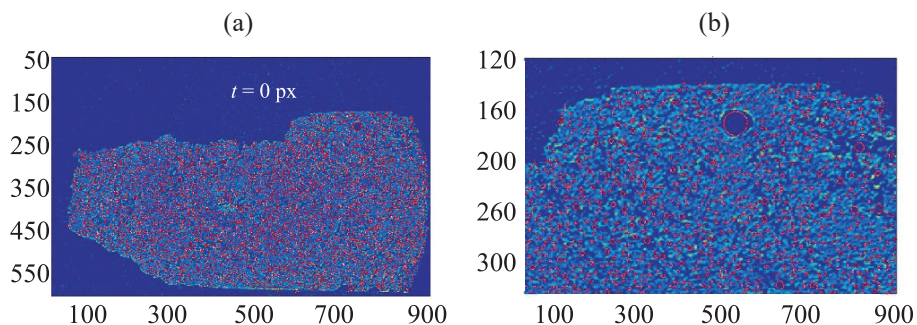


**Fig. 5.** Image of a cross-section of a sample of irradiated GR-220 graphite and maximum pore throat cross-sections (a) full cross-section of a sample and (b) magnified fragment of the sample cross section.

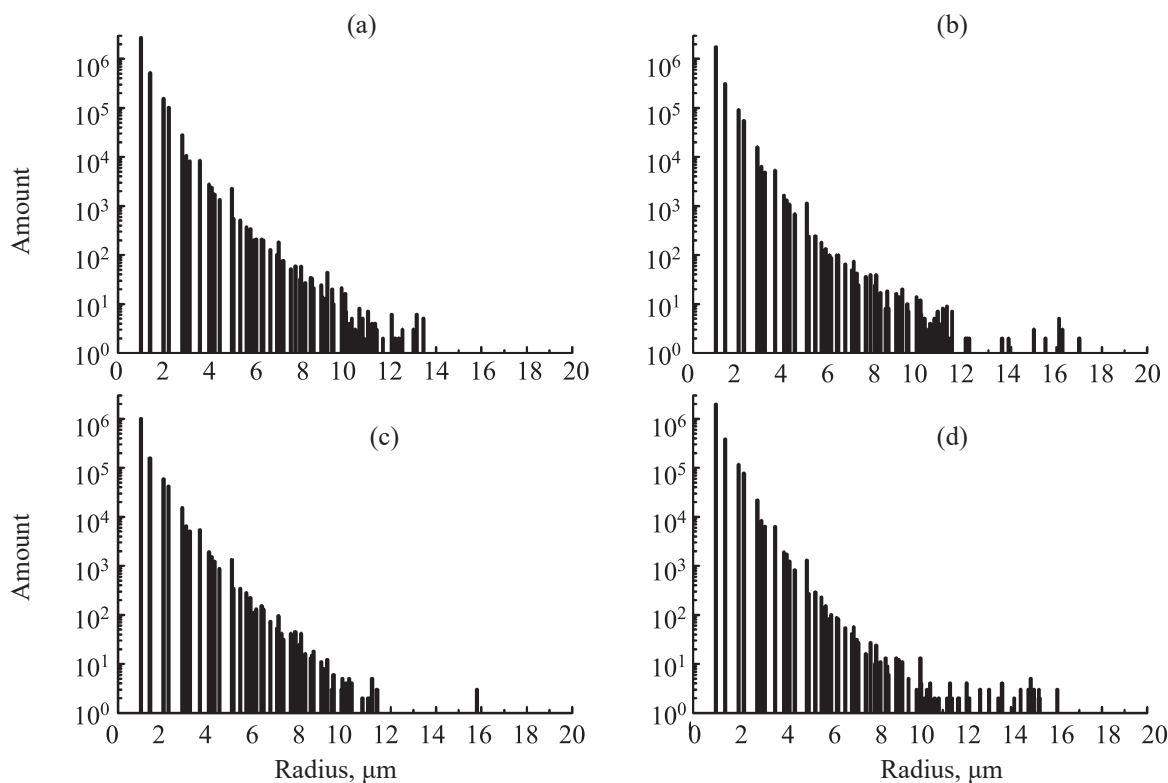


**Fig. 6.** Radii of the maximum pore throat cross-section and results of a calculation of the average radius of the throat cross-section: (a) GR-220 (block) virgin,  $R_{av} = 8.90 \mu\text{m}$ , (b) GR-220 irradiated,  $R_{av} = 8.78 \mu\text{m}$ , (c) GR-76 (bushing) virgin,  $R_{av} = 9.10 \mu\text{m}$ , (d) GR-76 irradiated,  $R_{av} = 8.91 \mu\text{m}$ .

from  $\sim 10$  to  $40\text{--}60$  nm, which is close to the conclusions made in [23]. It is noteworthy, however, that the same size range is characteristic of vacancy aggregations in various kinds of irradiated graphite [24], and it is quite probable that these defects make a significant contribution to the intensity of SAXS.

With reservation the block graphite may be described as a so-called hierarchical system of scatterers, i.e., two independent types of heterogeneities are present. This

is indicated by weak inflections at about  $q = 0.4$  and  $0.75 \text{ nm}^{-1}$ . If one of these subsystems is attributed to the nanopores (typical case in carbon adsorbents), then the gyration (inertia) radius of these pores is  $\sim 1.3$  nm for the block graphite and  $1.4$  nm for the virgin and  $1.5$  nm for irradiated bushing graphite. However, a calculation of the volume fraction of pores from the small-angle scattering data is rather ambiguous [25]. Comparison of the data of X-ray tomography and small-angle scattering

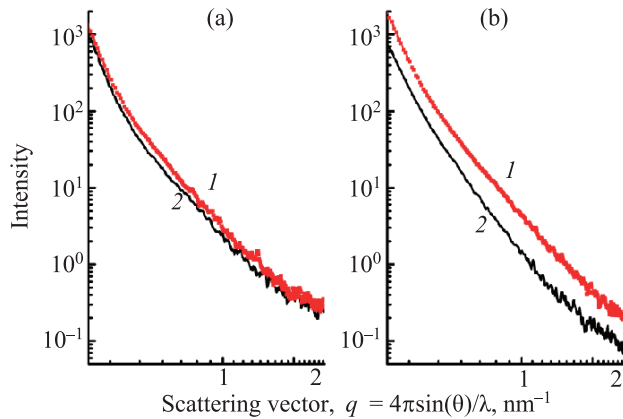


Fig. 7. Small-angle scattering curves for the studied samples. (a) GR-220 and (b) GR-76. Virgin (1) and irradiated (2).

shows that changes in the porous structure in the course of irradiation of the samples under study are rather small.

## DISCUSSION

The results of this work demonstrate properties of the porous structure such as the size distribution of pore throats and the average radius do not differ significantly between the studied graphite brands. Reactor irradiation (even during the whole service life for GR-220) do not lead to statistically significant changes in these parameters.

If we consider the porous structure of graphite as a network of interconnected channels with round cross-section, then their surface area can be estimated by the formula

$$F_S = \frac{2vV}{r}, \quad (4)$$

where  $v$  is the volume fraction of open pores in graphite,  $V$  is the sample volume,  $\text{cm}^3$ ;  $r$  is the average radius of the cross-section of open pores,  $\text{cm}$ .

According to Eq. (4), for the studied graphite brands at average pore radius  $r \approx 9 \mu\text{m}$  (Fig. 6), average volume of open porosity  $v \approx 0.17$  and density of  $\sim 1.7 \text{ g/cm}^3$ , the specific (per unit mass) surface area of open pores,  $F_S$ , is  $\sim 225 \text{ cm}^2/\text{ton}$ . It should also be noted that the pores are irregularly shaped, and the  $r$  is the radius of the maximum round throat inscribed in a real cross-section (Fig. 5). Therefore, the real value will be somewhat larger. Fine pores with size smaller than the resolution of the tomographic experiment also contribute to underestima-

tion of the calculated value. For samples with volume of  $\sim 1 \text{ cm}^3$  (such sample of irradiated graphite are the most frequently used in leaching tests equation (4) shows that the open pore volume  $F_S$  is  $\sim 380 \text{ cm}^2$ . In this case, the surface area of the sample is (depending on its shape)  $F_0 \approx 4.5\text{--}6 \text{ cm}^2$ . Thus, the surface area of open pores,  $F_S$ , strongly (by nearly two orders of magnitude) exceeds the outer surface area of the samples,  $F_0$ . With increasing volume of a sample (fragment of graphite RAW) the  $F_S/F_0$  ratio will only grow.

On the assumption that the whole open-pore volume (or its significant part) in a sample is filled by the leaching solution and  $F_S \gg F_0$ , Eq. (3) can be written as

$$R_{\text{eff}n}^i = \frac{a_n^i}{A^i F_S t_n}.$$

Thus, the effective leaching rate  $R_{\text{eff}n}^i$  will be determined by the porous-structure characteristics (surface of open pores,  $F_S$ , specific activity of graphite,  $A^i$ , and activity  $a^i$  of radionuclides that passed into solution during  $n$ th period  $t_n$  of leaching.

## CONCLUSIONS

It was shown that nearly the whole volume of pores (including internal domains) in both virgin and irradiated graphite of the studied brands is open and accessible for saturation with water when kept in an aqueous medium. A tendency is observed towards an insignificant decrease in the fraction of open porosity during reactor operation. With consideration for the initial variation of this quantity, a decrease of not more than 25% is observed for block graphite GR-220 and by 15% for the bushing graphite GR-76. A probable explanation is that the graphite lattice swells because of the accumulation of radiation defects. The open-pore surface area for graphite of the studied brands strongly (by more than two orders of magnitude) exceeds, even in the case of small ( $\sim 1 \text{ cm}^3$ ) volumes of graphite, the surface area of graphite fragments. This fact indicates that the leaching process of the main long-lived radionuclides in the graphite bulk is close to the volume one. The contribution of the open pore surface to the rate of the leaching process will dominate over that of the outer surface of the fragments.

At evaluation of factors characterizing the resistance against leaching of radionuclides it is necessary to take into account developed structural porosity of



graphite and the volume character of the distribution of radionuclides. For this purpose, two parameters: the effective leaching surface area  $F_{\text{eff}}$  and effective leaching rate  $R_{\text{eff}}$ , were introduced. In the framework of the proposed model of the leaching process, the parameter  $R_{\text{eff}}$  determines the stability of the material (irradiated graphite) against leaching and is independent of the geometric characteristics of the sample/fragment.

It should be noted, that the suggested model of radionuclide leaching from irradiated graphite is valid when the following conditions are fulfilled:

– the process of filling of all the accessible cavities in the graphite structure (pores, intercrystallite spaces, etc.) by the contact solution is complete and, accordingly, the effective leaching surface area stabilizes;

– intensity of mass exchange between the leaching solution in the volume of pores with the volume over the outer surface of the graphite fragment stabilizes;

– rate of sorption/desorption of radionuclides in the course of their propagation along pore channels to the fragment surface attained equilibrium.

To verify the adequacy of the suggested model, the authors are performing a series of experiments on prolonged leaching of radionuclides on real samples of graphite RAW of various brands and configurations. The results of this work will be used in calculations for estimating the long-term dynamics of rate of release of radionuclides in the course of leaching from graphite RAW of various types in the possible variants of the disposal.

#### ACKNOWLEDGMENTS

The study used the equipment of the Center for collective use of physical research methods at the Institute of Physical Chemistry and Electrochemistry, Russian Academy of Sciences. The authors are grateful to A.V. Buzmakov for assistance in processing of tomographic data.

#### FUNDING

The study of the leaching was in part supported by the Program no. 14P of the Presidium of the Russian Academy of Sciences. The processing of the tomographic data was supported by the Ministry of Science and Higher Education under the State assignment to the Federal Research Scientific Center “Crystallography and Photonics”, Russian Academy of Sciences.

#### CONFLICT OF INTEREST

The authors state that they have no conflict of interest.

#### REFERENCES

- Dorofeev, A.N., Komarov, E.A., Zakharova, E.V., Volkova, A.G., Martynov, K.V., Linge, I.I., Ivanov, A.Yu., Utkin, S.S., Pavlyuk, A.O., and Kotlyarevskii, S.G., *Radioaktivnye Otkhody*, 2019, no. 2(7), p. 18. <https://doi.org/10.25283/2587-9707-2019-2-18-30>
- IAEA TECDOC no. 1790 “Processing of Irradiated Graphite to Meet Acceptance Criteria for Waste Disposal. Results of a Coordinated Research Project,” Vienna: IAEA, 2016.
- Wickham, A., Steinmetz, H.-J., O’Sullivan, P., and Ojovan, M.I., *J. Environ. Radioact.*, 2017, vol. 171, p. 34.
- <https://www.cambridge.org/core/journals/radiocarbon/issue/B16E687954999C131670CC8705D8A2B0>
- Bushuev, A.V., Kozhin, A.F., Petrova, E.V., Zubarev, V.N., Aleeva, T.B., and Girke, N.A., *Radioaktivnyi reaktornyi grafit* (Radioactive Reactor Graphite), Moscow: MIFI, 2015.
- Pavlyuk, A.O., Kotlyarevskii, S.G., Markov, S.A., and Shatrov, M.V., *Radioaktivnye Otkhody*, 2018, no. 3(4), p. 69.
- Pavlyuk, A.O., Kotlyarevskii, S.G., Bepala, E.V., Volkova, A.G., and Zakharova, E.V., *Izv. Tomsk. Politekhn. Univ., Inzhiniring Georesurov*, 2017, no. 328(8), p. 24.
- Volkova, A.G., Zakharova, E.V., Pavlyuk, A.O., and Shiryayev, A.A., *Radiochemistry*, 2018, vol. 60, no. 5, p. 558. <https://doi.org/10.1134/S1066362218050144>
- Volkova, A.G., Zakharova, E.V., Rodygina, N.I., Pavlyuk, A.O., and Shiryayev, A.A., *Radiochemistry*, 2018, vol. 60, no. 6, p. 657. <https://doi.org/10.1134/S1066362218060152>
- Bepala, E.V., Pavlyuk, A.O., Zagumenov, V.S., Kotlyarevskii, S.G., *Izv. Vuzov. Yadern. Energetika*, 2017, no. 4, p. 116. <https://doi.org/10.26583/npe.2017.4.11>
- Shiryayev, A.A., Volkova, A.G., Zakharova, E.V., Nikol’skii, M.S., Averin, A.A., Dolgoplova, E.A., and Yapaskurt, V.O., *Radiochemistry*, 2018, vol. 60, no. 6, p. 664. <https://doi.org/10.1134/S1066362218060164>
- Vukovic, F., Leyssale, J.-M., Aurel, P., Marks, N.A., *Phys. Rev. Appl.*, 2018, vol. 10, no. 6, p. 064040. <https://doi.org/10.1103/PhysRevApplied.10.064040>
- Gurovich, B.A. and Prikhodko, K.E., *Radiat. Effects Defects Solids*, 2001, vol. 154, no. 1, p. 39.

- <https://doi.org/10.1080/10420150108214042>
14. Nicaise, G.O. and Poncet, B., *Kerntechnik*, 2016, vol. 81, no. 5, p. 565.  
<https://doi.org/10.3139/124.110732>
  15. Virgil'ev, Yu.S., *Khim. Tverd. Topliva (Solid Fuel Chemistry)*, 2000, no. 2, p. 67.
  16. Virgil'ev, Yu.S., *Khim. Tverd. Topliva (Solid Fuel Chemistry)*, 1973, no. 5, p. 102.
  17. Kane, J.J., Carroll, M., and Windes, W.E., *Int. Nuclear Graphite Specialists' Meeting INGS-17. IAEA, Sept. 4-8, 2016*.
  18. Laudone, G.M., Gribble, C.M., and Matthews, G.P., *Carbon*, 2014, vol. 73, p. 61.  
<https://doi.org/10.1016/j.carbon.2014.02.037>
  19. GOST (State Standard) 29114-91. *Otkhody radioaktivnye. Metod izmereniya khimicheskoi ustoychivosti otverzhdennykh radioaktivnykh otkhodov posredstvom dlitel'nogo vyshchelachivaniya* (Radioactive Waste. A Method for Measuring the Chemical Stability of Solidified Radioactive Waste by Long-Term Leaching.).
  20. GOST 52126-2003. *Opreделение khimicheskoi ustoychivosti otverzhdennykh vysokoaktivnykh otkhodov metodom dlitel'nogo vyshchelachivaniya* (Determination of the Chemical Stability of Solidified High-Level Waste by the Long-Term Leaching Method.).
  21. Shiryaev, A.A., Kaminsky, F.V., Ludwig, W., Zolotov, D.A., Buzmakov, A.V., and Titkov, S.V., *Geochem. Int.*, 2019, vol. 57(9), p. 1015.
  22. GOST 18898-89. *Izdeliya poroshkovye. Metody opredeleniya plotnosti, soderzhaniya masla i poristosti* (Powder Products. Methods for Determining Density, Oil Content, and Porosity).
  23. Virgil'ev, Yu.S., Kurolenkin, E.I., and Shurshakova, T.N., *Izv. Akad. Nauk SSSR, Neorgan. Mater.*, 1977, vol. 13, no. 4, p. 752.
  24. Shtrombakh, Ya.I., Gurovic, B.A., Platonov, P.A., and Alekseev, V.M., *J. Nucl. Mater.*, 1995, vol. 225, p. 273.  
[https://doi.org/10.1016/0022-3115\(95\)00060-7](https://doi.org/10.1016/0022-3115(95)00060-7)
  25. Shiryaev, A.A., Voloshchuk, A.M., Volkov, V.V., Averin, A.A., and Artamonova, S.D., *J. Phys.: Conf. Ser.*, 2017, vol. 848, p. 012009.